

Bits-to-Photon: End-to-End Learned Scalable Point Cloud Compression for Direct Rendering

Yueyu Hu¹, Ran Gong^{1,2}, and Yao Wang¹

¹ Dept. Electrical and Computer Engineering, New York University, Brooklyn, NY

² Tsinghua University, Beijing, China
{yyhu, rg4827, yaowang}@nyu.edu

Abstract. Point cloud is a promising 3D representation for volumetric streaming in emerging AR/VR applications. Despite recent advances in point cloud compression, decoding and rendering high-quality images from lossy compressed point clouds is still challenging in terms of quality and complexity, making it a major roadblock to achieve real-time 6-Degree-of-Freedom video streaming. In this paper, we address this problem by developing a point cloud compression scheme that generates a bit stream that can be directly decoded to renderable 3D Gaussians. The encoder and decoder are jointly optimized to consider both bit-rates and rendering quality. It significantly improves the rendering quality while substantially reducing decoding and rendering time, compared to existing point cloud compression methods. Furthermore, the proposed scheme generates a scalable bit stream, allowing multiple levels of details at different bit-rate ranges. Our method supports real-time color decoding and rendering of high quality point clouds, thus paving the way for interactive 3D streaming applications with free view points.

Keywords: Scalable Point Cloud Compression · Point Cloud Rendering · 3D Sparse Convolution

1 Introduction

Volumetric video streaming is a promising technology with the recent advancement of AR/VR devices. It allows users to view a 3D scene with 6 degrees of freedom (6-DoF) while the scene changes in time. It is expected to revolutionize both the way we communicate and entertain. However, since the 3D scene needs to be captured, transmitted, and rendered in real time, it inevitably incurs high requirements in network bandwidth and computation resources.

To reduce the consumption of bandwidth and alleviate the computational burden of surface reconstruction, point clouds have been recognized as a form of promising 3D representation for volumetric streaming in emerging AR/VR applications [12, 19], given the flexibility in capturing and compression of point clouds. Tremendous progress has been made in the past few years in point cloud compression, including the MPEG Point Cloud Compression (PCC) standards [21] and recent deep learning based methods [14, 26, 31]. These methods are typically

developed to compress either the geometry (point coordinates) or color, and have shown great potential in compressing point clouds to a low bit-rate. However, there remains a gap between the reconstruction of point cloud and the rendering of high-quality images on the clients' display. The color compression methods are mostly optimized to accurately reproduce the point-wise colors, rather than the rendering quality. As a result, the rendering quality from the compressed point clouds using standard rendering tools is sometimes severely compromised with visible holes and color artifacts. Although the state-of-the-art learned point cloud rendering method [4] can improve the rendering quality, it is very slow and cannot support real-time free viewpoint.

In this paper, we propose a point cloud compression scheme that generates a bit stream that can be directly decoded to 3D Gaussians, which can then be rendered efficiently and with high quality using Gaussian splatting [18]. The encoder and decoder are end-to-end optimized towards lower bit-rates and better rendering quality. It allows multiple levels of details at different bit-rate ranges and significantly improves the rendering quality at similar bit-rates, while substantially reducing the decoding and rendering time compared to existing separate point cloud compression and rendering methods. Our method supports real-time color decoding and rendering of high quality point clouds, paving the way towards building interactive 3D streaming applications with free view points.

Since the scalable coding of point cloud geometry has been well studied in the work of SparsePCGC [25], in this paper we focus on coding the color and other rendering related information in a scalable stream. Following the octree coding structure, we first extract features at different levels of the octree. We then compress the features using a hierarchical coding scheme, where the entropy coding at each level is conditioned on the up-sampled features from the previous coarser level. The feature bits at each level are decoded directly to 3D elliptical Gaussians with opacity and color, which can then be efficiently rendered to arbitrary view points using the Gaussian splatting technique [18, 29, 34]. The proposed approach thus allows multiple levels of details at different bit-rate ranges.

Our feature extraction and compression and decompression modules are built upon the sparse 3D convolutional neural network based on the Minkowski Engine [6]. We propose a novel geometry-invariant 3D sparse convolution to address the problem of non-uniform density in the point cloud, which is crucial for color feature extraction and reconstruction. With the help of a differential renderer leveraging the 3D Gaussian representation, we can end-to-end optimize the encoder and decoder jointly towards better rendering quality and lower bit-rates.

We train our model on the training set of the THuman 2.0 dataset [30], which contains point clouds of full-body human in action. We evaluate our method on the testing set of the THuman 2.0 dataset and the 8i Voxelized Full Bodies (8iVFB) dataset [8]. Our method achieves higher perceptual quality (substantially higher in terms of PSNR) in the rendered images at similar bit rates as G-PCC v22 and the state-of-the-art deep learning based point cloud attribute compression method [9]. Meanwhile, our color decoding (using GPU) is sub-

stantially faster than both G-PCC (using CPU, cannot benefit from GPU) and the learning-based method (using GPU), at 10s of milliseconds (ms) per frame, compared to seconds. Although the state-of-the-art learned geometry decoding method that we leverage [25] is still at 100s of ms, our method for coding the color and rendering-related information paves the way for future real-time volumetric video streaming applications.

- We propose a novel end-to-end learned point cloud compression method that directly decodes bit-streams to renderable 3D Gaussians, bridging the gap between point cloud compression, reconstruction, and rendering. Leveraging a differentiable renderer utilizing Gaussian splatting, we directly optimize the rendering quality vs. bit-rate trade-off.
- We adapt sparse convolution for feature extraction, squeezing, conditional entropy coding, and reconstruction. We propose a novel geometry-invariant 3D sparse convolution to address the problem of non-uniform point density in the point cloud.
- We propose a novel hierarchical coding scheme for the compressing the color and rendering-related information. It generates a scalable bit-stream and allows multiple levels of details at different bit-rate ranges. Our method (B2P) significantly improves the rendering quality at similar bit-rates compared to both standard and learned methods for point cloud color compression, while substantially reducing the decoding and rendering time.

2 Related Works

2.1 Point Cloud Compression

With the wide applications of point clouds in autonomous driving, AR/VR, and volumetric video capturing and streaming, point cloud compression has been an active research area in the past few years. The MPEG 3D Graphics Coding group has standardized the video-based (V-PCC) and the geometry-based point cloud codecs (G-PCC) [5, 11]. The V-PCC projects 3D point clouds to 2D images and encodes them by a standard video codec. It is efficient in terms of compression ratio especially for dynamic point clouds (*a.k.a.* point cloud videos (PCV)), but lacks level-of-detail (LoD) scalability and may introduce 3D artifacts in the reconstructed geometry. The G-PCC, on the other hand, encodes the geometry using an octree structure, with context-adaptive entropy coding. G-PCC stream is scalable, making it easy to adapt to time-varying network bandwidths in streaming applications. Given the coded geometry, it adopts the Region-Adaptive Hierarchical Transform (RAHT) to efficiently encode the color, achieving high rate-distortion performance.

With the advancement in 3D neural network architectures [6, 24, 28], neural network-based methods show great potential in boosting the rate-distortion performance in point cloud compression. One line of works focus on using neural networks to improve conditional entropy modeling on the octree structure for lossless geometry compression [7, 10, 15, 20, 22]. These works are particularly

optimized for compression of geometry and are not directly applicable to the color and other rendering related information. Another line of works focus on compressing point clouds sampled from a 3D surface, where the geometry is usually coded in the first place [14, 25, 27] and colors are coded conditioned on the decoded geometry [9, 23, 26, 31]. These methods demonstrate great potential in compressing point clouds to a low bit-rate while maintaining the color and geometry fidelity. However, all these methods compress geometry and color separately, unaware of the rendering quality tradeoff, and sometimes lead to visible holes and color artifacts in the rendered images. In this paper, we propose a novel end-to-end learned method that compresses the color and other rendering information, so that the decoded bit stream along with the geometry bits can be directly decoded to renderable 3D Gaussians, bridging the gap between point cloud compression, reconstruction, and rendering.

2.2 Differential Point Cloud Rendering

Our work is based on the key innovation of differential point cloud rendering [2, 4, 29], which allows us to optimize the bitrate-rendering-distortion tradeoff directly. Specifically, we are inspired by the work of 3D Gaussian splatting [18], which demonstrate that 3D Gaussian clouds are capable of representing a 3D scene with high fidelity and rendering images without holes. Their work focused on the generation of 3D Gaussians from given multi-view images of one scene through per-scene optimization. In this work, we tackle a different problem, where we are given a colored point cloud and aim to compress it to a low bit-rate while maintaining the rendering quality. Our key contributions are developing neural network modules to extract compact features from the point cloud, conduct entropy coding, and decode to 3D Gaussians for high-quality rendering.

3 Method

3.1 Hierarchical Compression and Rendering

We represent the point cloud geometry (*i.e.* the coordinates of all points) using an octree structure, which has been found to be efficient in representing the sparse structure of point clouds [16]. The octree is constructed by recursively subdividing the 3D space into 8 equal octants. Each node represents the occupancy of the corresponding octant. If one octant is completely empty, the corresponding node is marked unoccupied and not further subdivided. A point cloud where each coordinate is represented with N bits can be represented by an octree with N levels, where each leaf node represents an original point in the point cloud. The octree structure provides a hierarchical representation of the geometry of the point cloud, which naturally facilitates scalable compression and rendering with multiple levels of detail. It also allows us to efficiently find the neighbors of a point in the point cloud, which is crucial for sparse 3D convolutions.

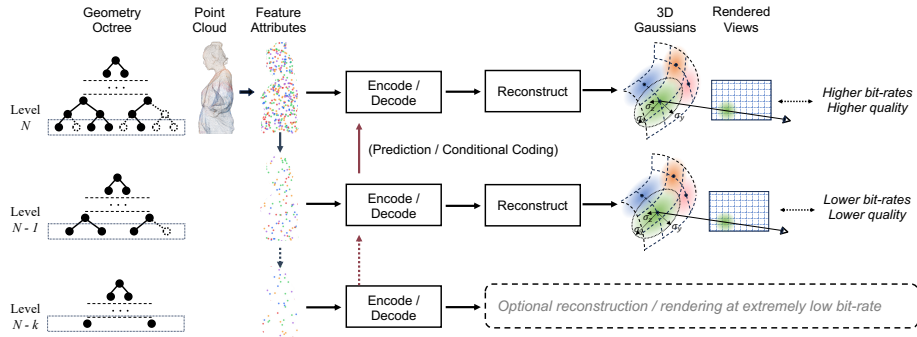


Fig. 1: Hierarchical Compression and Rendering framework.

With the octree geometry structure, we compress the point cloud by first losslessly encode the geometry using an existing scalable point cloud geometry compression method, such as SparsePCGC [25] or G-PCC [21], and then encode the color and other rendering related information given the geometry defined by the octree structure. The hierarchical compression and rendering pipeline is illustrated in Fig. 1.

We first extract color features¹ from the original point cloud at level N . We then generate hierarchical feature representation by repeatedly downsampling the extracted features following the octree structure, until a chosen level L , using the average pooling in a $2 \times 2 \times 2$ neighborhood. We then encode the features at different levels using a hierarchical coding scheme. We start with coding the color features at level L independently, and then code features at successive higher levels conditioned on the upsampled features from the lower level, until level N .

The hierarchical coding scheme naturally generates a scalable bit-stream, and allows us to achieve different bit-rates and different levels of details, by transmitting up to different levels M ($L \leq M \leq N$), with M chosen based on the sustainable network throughput between the sender and the receiver or the decoder processing constraint. We have observed that, when the geometry is too sparse (*i.e.*, M is too small), it is very hard for the features to carry enough information for rendering with adequate quality. We found that for a typical 10-bit point cloud ($N = 10$), the best rate-quality tradeoff is achieved by transmitting starting from level $L = 7$ up to level $M \in \{8, 9\}$ and rendering at level M . Although it is possible to transmit all way to level 10, the quality improvement from level 9 to level 10 does not justify the additional bits needed.

¹ For simplicity, we call these color features. But they actually carry additional information needed to recover the 3D Gaussians for rendering.

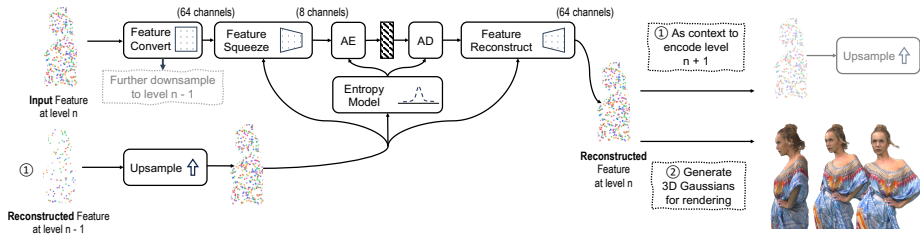


Fig. 2: Predictive entropy coding for level n , conditioned on the reconstructed feature at a coarser level $n - 1$.

We extract features at level N using a multi-layer Minkowski Convolution Network [6]. The original Minkowski convolution is defined as,

$$\mathbf{x}_u = \sum_{u+i \in \mathcal{N}(u, K, P^{\text{in}})} W_i \mathbf{x}_{u+i} \text{ for } u \in P^{\text{out}}, \quad (1)$$

where K is the kernel size and $\mathcal{N}(u, K, P^{\text{in}})$ is the set of occupied input points that are within the kernel size of the output point u . P^{in} and P^{out} denote the set of occupied points. We observe that this definition of convolution is not geometry invariant, as it tends to produce higher magnitude where the neighborhood around u is denser. To address this problem, we propose a geometry-invariant 3D sparse convolution, which is crucial for color feature extraction and reconstruction. The geometry-invariant 3D sparse convolution is defined as,

$$\mathbf{x}_u = \frac{1}{\sqrt{\sum_{u+i \in \mathcal{N}(u, K, C^{\text{in}})} W_i^2}} \sum_{u+i \in \mathcal{N}(u, K, C^{\text{in}})} W_i \mathbf{x}_{u+i} \text{ for } u \in C^{\text{out}}, \quad (2)$$

which normalizes the output response by the norm of **active** kernel weights. This normalization ensures that the convolution response is consistent across different point densities in the local area.

We detail the conditional entropy coding in Sec. 3.2 and the 3D Gaussian decoding in Sec. 3.3. Please refer to the supplementary material for more details on the network architectures we used to extract features and generate the 3D Gaussian clouds.

3.2 Feature Squeezing and Conditional Entropy Coding

We compress the features at each level using feature squeezing and conditional entropy coding, shown in Fig. 2. Suppose we are coding **input** features at level n , given **reconstructed** features already decoded at level $n - 1$. We first apply a feature squeezing module to reduce the number of input feature channels from 64 to 8. The motivation of feature squeezing is that the features at level n can usually be predicted well from features at level $n - 1$ and we only need to encode the *residual* information in level n , which is usually sparser and requires fewer channels to represent. The squeezing module learns to generate the *residual* in a

general sense given the context, and prepare the residual features for quantization and entropy coding. We use the Minkowski Inception ResNet architecture [27] with the proposed geometry-invariant 3D convolution for the squeezing module.

To encode the squeezed features, we first quantize the feature components to integers, and use a conditional arithmetic coder to encode the quantized features to binary bit-streams using the up-sampled features from the reconstructed features at level $n - 1$ as the conditioning context. During training, the quantization is simulated using additive uniform noise $U(-0.5, 0.5)$. Following the entropy coding method of [3], we assume the unquantized feature values follow a Gaussian distribution with spatially varying mean and variance, so that the probability of each quantized value x_u at point u is calculated as,

$$p(X = x_u) = \Phi(x_u + 0.5; \mu_u, \sigma_u) - \Phi(x_u - 0.5; \mu_u, \sigma_u), \quad (3)$$

where Φ is the Gaussian cumulative distribution function (CDF) and μ_u, σ_u are estimated from the context features. We assume the number of bits needed to code $X = x_u$ equals the negative log likelihood, as,

$$R(x_u) = -\log_2 p(X = x_u). \quad (4)$$

Hence, we define the bit-rate loss at level n as the sum of the bits for all points at this level P_n :

$$\mathcal{L}_R^n = \sum_{u \in P_n} -\log_2 p(x_u). \quad (5)$$

During inference, the arithmetic coder will utilize the estimated probability $p(X = x_u)$ from the context features to encode the value $X = x_u$, with a code length very close to (4).

After entropy coding, the quantized features are concatenated with the context features along the channel dimension, and go through the feature reconstruction module. This module produces the **reconstructed** features at level n , which serve two purposes: (1) It can be used as the context to encode the next level $n + 1$; (2) If we need to render at level n , we can generate the 3D Gaussian cloud directly from the reconstructed features. By encoding and decoding recursively across the scale using the proposed scheme, we achieve level-of-detail scalability, while reducing the total bit rate up to level N .

3.3 From Features to 3D Gaussians

The reconstructed features we obtain at each level are feature vectors attached to some grid points in the voxelized space. We convert the feature vectors at the highest level M that is transmitted and received to renderable 3D Gaussians. We use the differential Gaussian splatting renderer proposed in [18]. Each 3D Gaussian is parameterized by a center coordinate (*a.k.a.* the 3D means) (μ_x, μ_y, μ_z) , a covariance matrix Σ , an opacity value o , and a color triplet c . Since the features are extracted from the original point cloud that does not have anisotropic color, we simplify the original parameterization by using color $c \in [0, 1]^3$ instead of

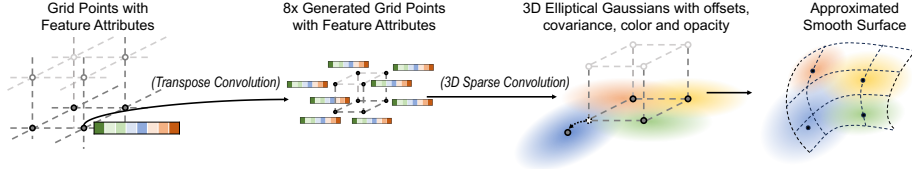


Fig. 3: Generative rendering.

the spherical harmonics. Each 3D Gaussian is then rendered to the screen space using the splatting technique, and the rendered colors by overlapping Gaussians are combined using alpha blending. A pixel in the screen space is shaded as color C , where,

$$C = \sum_{k=1}^K T_k \alpha_k c_k, \quad (6)$$

where α_k is the opacity of the k -th splat, and $T_k = \prod_{j=1}^{k-1} (1 - \alpha_j)$. The opacity α_k is calculated by projecting the 3D Gaussian onto the screen space and evaluate the Gaussian density at the projected pixel, weighted by the estimated opacity value o_k ,

$$\alpha_k = o_k \cdot e^{-\frac{1}{2} \mathbf{d}_k^T \Sigma_{k(s)}^{-1} \mathbf{d}_k}, \quad (7)$$

where $\Sigma_{k(s)}$ denotes the screen space covariance matrix and \mathbf{d}_k is the distance vector between the pixel and the Gaussian center in the screen space. The screen space covariance matrix $\Sigma_{k(s)}$ can be approximated as,

$$\Sigma_{k(s)} = \mathbf{J} \mathbf{R}_c \Sigma_k \mathbf{R}_c^T \mathbf{J}^T, \quad (8)$$

where \mathbf{J} is the Jacobian matrix of the projection from the 3D space to the screen space, and \mathbf{R}_c is the rotation matrix of the camera. We follow the parameterization of the 3D Gaussian as in [18], where the covariance matrix is parameterized as $\Sigma = \mathbf{R}^T \mathbf{S}^T \mathbf{S} \mathbf{R}$, where \mathbf{R} is a rotation matrix and $\mathbf{S} = \text{diag}(\sigma_x, \sigma_y, \sigma_z)$ is a diagonal matrix. This parameterization guarantees Σ to be positive semi-definite. The rotation matrix \mathbf{R} is calculated from a quaternion $\mathbf{q} = (q_w, q_x, q_y, q_z)$. The conversion from the reconstructed features to 3D Gaussians is in effect generating the following 14 parameters, $\mu_x, \mu_y, \mu_z, \sigma_x, \sigma_y, \sigma_z, q_w, q_x, q_y, q_z, o, c$, for all non-empty points.

A simple approach for this conversion is just to use the grid coordinates of the points as the 3D means, and predict the remaining parameters from the features. However, this simple approach has two limitations. First, the number of grid points decrease exponentially with the level of the octree. At a coarse level there might not be enough Gaussians to render the fine-grained texture of the 3D scene. Second, at a coarse level the grid coordinates may not be the correct center positions due to octree-based downsampling. Therefore, we propose a generative rendering scheme, shown in Fig. 3. The key idea is to generate more points from the original grid points, while allowing the module learning to disable falsely generated points by setting the opacity $o \rightarrow 0$. For each grid point

with a feature vector, we generate features at 8 sub-points using the generative transpose 3D convolution. The features at all subpoints are then converted to predicted Gaussian parameters, including the coordinate offsets $(\delta_x, \delta_y, \delta_z)$, and other parameters $\sigma_x, \sigma_y, \sigma_z, q_w, q_x, q_y, q_z, o, c$. The coordinate offsets are added to the grid point coordinates to produce the 3D means (μ_x, μ_y, μ_z) . Using the information carried by the feature, the module learns to enable or disable (by setting opacity value close to 0) the sub-points and move them to the correct positions through the predicted offsets to represent the underlying textured smooth surface.

In practice for $N = 10$, we found that this generative prediction is helpful at level $N - 2$ or lower. But at level $N - 1$ and N , we just need to predict one Gaussian for each non-empty point while setting the opacity of all Gaussians to a constant of 1. For each Gaussian, we predict the offset from the original grid coordinates and other parameters including $\sigma_x, \sigma_y, \sigma_z, q_w, q_x, q_y, q_z, c$.

3.4 Training

With the hierarchical coding structure and the scalable delivery and rendering scheme, we encode the point cloud into bit-streams at levels L to N , and depending on the target bit rate, deliver from level L up to level M and render at level M , with $L \leq M \leq N$. As mentioned earlier, some lower levels are too sparse for adequate rendering, thus they are only used for the conditional coding purpose. Therefore, we have $M > L$ in general.

Because we want to design a scalable coding scheme that can accommodate a large rate range corresponding to deliver up to a level between M_{\min} and M_{\max} , we train the model using the rate-distortion loss function defined on all coding and rendering levels, as,

$$\mathcal{L} = \sum_{n \in \{L, \dots, M_{\max}\}} \mathcal{L}_R^n + \lambda \sum_{n \in \{M_{\min}, \dots, M_{\max}\}} \mathcal{L}_D^n, \quad (9)$$

where the bit-rate term \mathcal{L}_R^n is defined as in Eq. (5) for level n . The distortion loss \mathcal{L}_D^n includes the weighted L1 distance, the SSIM loss, and the LPIPS loss [32], calculated between the rendered images \hat{x}^n at level n and the ground truth views x obtained by rasterizing the mesh provided in the training dataset, defined as

$$\mathcal{L}_D^n = \alpha \|x - \hat{x}^n\|_1 + \beta (1 - \text{SSIM}(x, \hat{x}^n)) + \gamma \mathcal{L}_{\text{LPIPS}}(x, \hat{x}^n). \quad (10)$$

During training, we calculate the loss function using 4 random views rendered from a scene. We set $\alpha = 3$, $\beta = 0.2$, and $\gamma = 1$ in our experiments. Note that to achieve more fine-grained rate control, besides the level scalability, we also train different models with different λ . We set $\lambda \in \{5, 10, 20\}$ in our experiments. It thus produces 3 sets of scalable bit-streams. As described earlier, for $N = 10$, we choose $M_{\min} = 8$ and $M_{\max} = 9$, because they lead to better rate-quality trade-offs and adequate rendering quality. Thus each scalable bit stream obtained by a model trained with a given λ has 2 rate-quality points, realizing a total of 6 Rate-Quality points. We use the Adam optimizer with a learning rate of 10^{-4} and a

batch size of 4. We train the model for 60,000 iterations on a single NVIDIA A100 GPU.

4 Experiments

4.1 Settings

We leverage the THuman 2.0 dataset [30] for training and testing, and also evaluate our trained models on the 8i Voxelized Full Bodies (8iVFB) dataset [8]. The THuman 2.0 dataset provides 525 meshes built from RGBD captures with human subjects performing actions. We densely sample the meshes to obtain the color point clouds, and use the point clouds to train and evaluate our model. The dataset is divided into a training set of 500 meshes (0000 – 0499) and the rest for testing, this guarantees a cross-subject validation with the testing set containing only unseen subjects. In our experiments, we report results with 8 point clouds from unrepeating subjects, namely {0507, 0509, 0511, 0513, 0515, 0517, 0519, 0521}. To evaluate the generalizability, we also test on the MPEG CTC 8iVFB dataset, which provides 4 full-body human point clouds in bit-depth 10, which can be represented losslessly by a 10-level octree.

We evaluate the following compression schemes:

- **G-PCC**. We use the MPEG G-PCC reference software TMC13v22 [1] to encode both the geometry (using octree) and the color (using RAHT). It varies the geometry quantization scale and color quantization parameters to achieve different bit-rates. We use the default settings for geometry and color quantization.
- **Learned** baseline. We use the state-of-the-art deep learning based scalable point cloud geometry compression method SparsePCGC [25] to encode the geometry, and use the learned point cloud attribute compression method 3DAC [9] to encode the color.
- **B2P (G-PCC)**. We use our method to compress the point cloud, given geometry coded by G-PCC up to a required level. We use the same settings as the G-PCC method for geometry coding, and use our method for color coding.
- **B2P (SpPCGC)**. Same as above but we replace the geometry coding with the state-of-the-art deep learning based scalable point cloud geometry compression method SparsePCGC [25].

We report bit-rates in bit-per-point (bpp), using the number of points from the original point cloud. We evaluate the rendering distortion at different bit-rates for comparison. We average the rendering distortion over 12 camera views forming a circle with equal angle intervals around the subject. Our decoder operation includes entropy decoding the squeezed features, reconstructing the features, and generating the Gaussian parameters, which can then be used to efficiently produce the rendered images given the camera extrinsics and intrinsics. For the G-PCC and the learned baseline, we first decode the point cloud, and

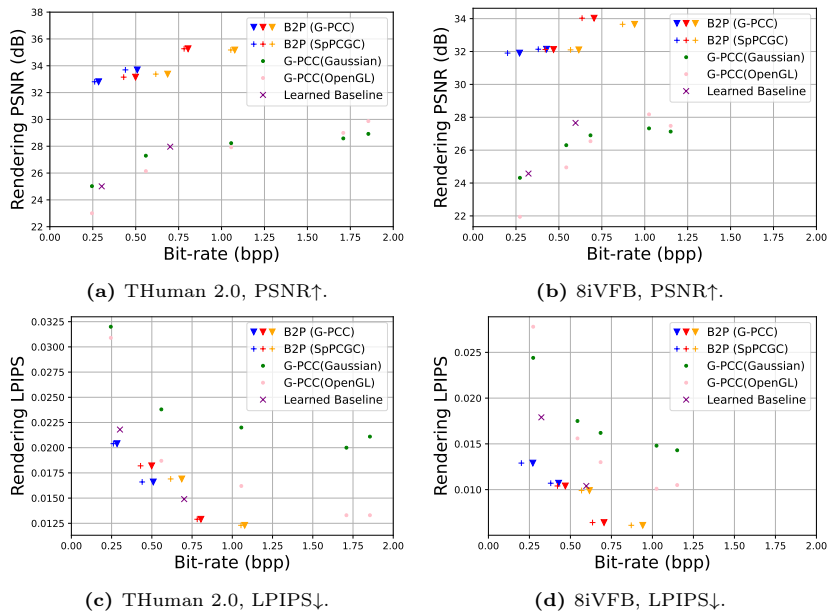


Fig. 4: Rendering distortion at different bit-rate by the proposed Bits-to-Photon (B2P) and baseline methods. We train 3 models with different λ values. Each model has 2 levels of scalability, forming 3 groups of scalable R-D points, plotted using different colors. Other methods are not scalable.

then render with the existing standard point cloud renderer provided by OpenGL and packaged in Open3D [33], which rasterizes each point as a solid square in the camera plane. We set the square size according to the point density so there is no visible hole. We also include an alternative renderer, taking each point as a spherical Gaussian with a global covariance matrix $\Sigma = \text{diag}(\sigma, \sigma, \sigma)$, where $\sigma = \bar{d}$ corresponding to the average nearest point distance. Since THuman 2.0 dataset provides ground truth meshes, we evaluate the rendering quality using the PSNR, MS-SSIM, and the LPIPS [32] between the rendered images from the decoded point clouds and the same views rendered from the ground truth meshes using standard rasterization. For the 8iVFB dataset which does not provide ground truth meshes, we first use the Screened Poisson surface reconstruction [17] to convert the point clouds to the meshes, and then render the meshes to produce ground truth images.

4.2 Rate-Distortion Performance

We plot the R-D points achieved by the proposed Bits-to-Photon (B2P) and compared methods in Fig. 4. As shown by the PSNR evaluation, images rendered by our method from our decoded bit-stream have more pixel-level fidelity to the ground truth images rendered from the mesh, with over 4 dB improvements in PSNR at the same level of bit-rate over the compared methods. We

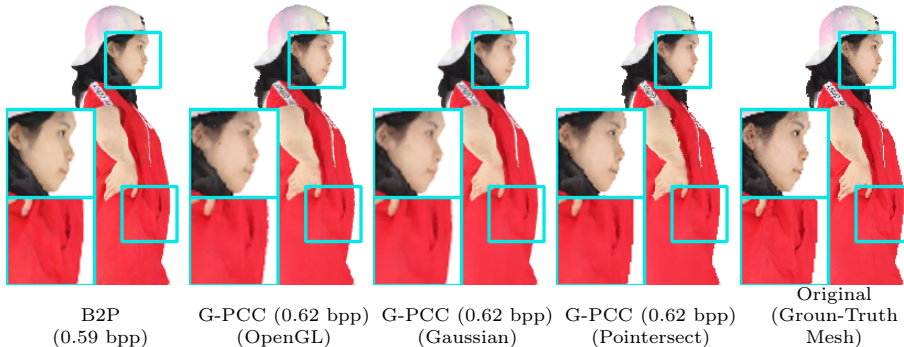


Fig. 5: Visual results on the decoded and rendered point cloud on the THuman 2.0 dataset, compared to images rendered from the ground truth mesh.

Table 1: Bit-rate and rendering quality at different octree levels and with different methods. We show averaged results over the 4 point clouds in the 8iVFB dataset.

Codec	Level	Renderer	bpp	PSNR \uparrow	LPIPS \downarrow	MS-SSIM \uparrow	Decode Time		Render Time
							Geometry	Color	
B2P (SpPCGC)	8	-	0.45	32.1	0.010	0.9948	270 ms	26 ms	4 ms
G-PCC	9	Gaussian	0.54	25.0	0.016	0.9824	2 sec		3 ms
G-PCC	9	Pointersect	0.54	29.4	0.010	0.9934	2 sec		1 sec
Learned	8	OpenGL	0.32	24.6	0.017	0.9703	270 ms	1 sec	2 ms
B2P (SpPCGC)	9	-	0.66	34.0	0.006	0.9967	370 ms	73 ms	5 ms
G-PCC	9 ⁺ ²	Gaussian	0.68	26.5	0.016	0.9854	4 sec		3 ms
G-PCC	9 ⁺ ²	Pointersect	0.68	29.8	0.010	0.9939	4 sec		1 sec
Learned	9	OpenGL	0.60	27.7	0.010	0.9893	370 ms	1 sec	3 ms

also show the results using LPIPS as the distortion metric, which is more sensitive to texture similarity and more tolerant to pixel-wise difference. Despite the disadvantage of Gaussian based renderer over OpenGL in terms of sharpness, our method still achieves better rate-distortion tradeoffs. We note that, from the R-D curves presented, B2P with $\lambda = 20$ (orange points) is not an appropriate choice, yielding higher rates at similar quality compared to $\lambda = 10$. In Fig. 5 and 6, we demonstrate better visual quality with finer facial details, sharper edges and higher contrast at a lower bit-rate, compared to G-PCC.

4.3 Bit-rate, Complexity, and Distortion Tradeoff

In a volumetric streaming system, there is usually a tradeoff among the bandwidth consumption, decoding and rendering complexity, and the rendering quality. We study this tradeoff comparing the baseline methods and B2P with the 8iVFB dataset. Our evaluation is conducted on a desktop computer with an Intel i7-9700K CPU and an NVIDIA RTX 4080 Super GPU. B2P, SparsePCGC, Global-Parameter Gaussian-based rendering, 3DAC and Pointersect are using

² Using geometry quantization scale 0.75.

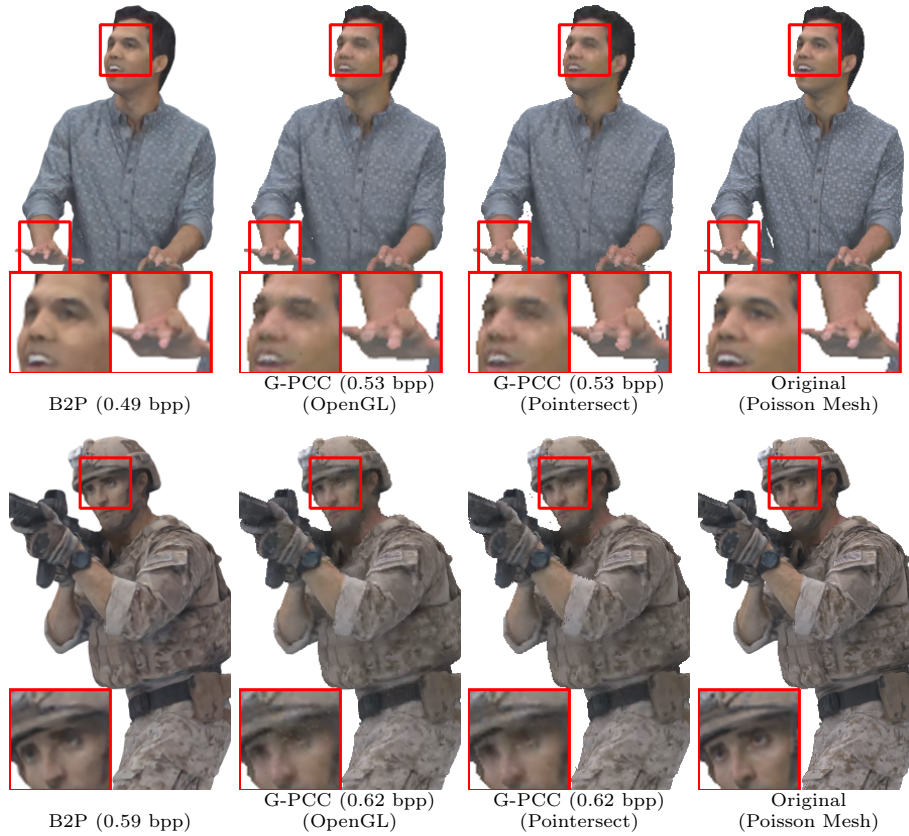


Fig. 6: Visual results on the decoded and rendered point clouds on the SiVFB dataset, compared to images rendered using the generated meshes from original point clouds.

both CPU and GPU, where the neural networks parts are running on GPU. G-PCC is running on CPU.

We show the benchmarking results in Table 1. As shown, B2P shows better R-D performance than compared methods at a lower decoding latency. We have the following observations:

- B2P decoding and rendering at octree level 8 already achieves better R-D performance than G-PCC at level 9. Although given a better point cloud renderer (Pointersect), the rendering distortion can be further reduced with the same reconstructed point cloud from G-PCC, the rendering complexity is too high for a real-time 6-DoF display.
- Learning based codec achieves better R-D performance than G-PCC, but the color coding part (3DAC) is still very complex.
- B2P provides better rendering quality by further decode one more level in the octree, as an enhancement layer. Although the decoding time will increase (but still substantially lower than G-PCC and 3DAC), since B2P is scalable, we may conduct region-adaptive enhancement layer decoding in a

Table 2: Average bit-rate (bpp) for color feature coding at different levels and λ .

Dataset	$\lambda = 5$			$\lambda = 10$			$\lambda = 20$		
	Level 7	Level 8	Level 9	Level 7	Level 8	Level 9	Level 7	Level 8	Level 9
THuman 2.0	0.049	0.136	0.010	0.053	0.333	0.092	0.057	0.509	0.182
SiVFB	0.037	0.164	0.007	0.040	0.358	0.086	0.043	0.503	0.175

real application and achieve a better tradeoff between complexity and R-D performance. We leave this as a promising future work.

We further analyze the bit-rate consumption by B2P at each of the hierarchical coding levels (7, 8, and 9), shown in Table 2. We observe that level 8 generally takes the largest portion of the bits, while level 9 does not take as much. This suggests that there are more unpredictable information at level 8 from level 7 features, while level 9 features can be predicted from level 8 features quite well. We will explore improvement of feature prediction from level 7 to level 8 as a future work. On the other hand, the unconditional coding at level 7 consumes about 10% of the bit-rate, but the portion is larger with a lower λ . This suggests that further improvements can be made to coding the coarser levels to improve performance at a lower bit-rate region.

5 Discussion of Limitations

In this paper, we show that it is promising to jointly design a point cloud compression scheme with a differentiable renderer for lower decoding and rendering latency, and better rate vs.rendering-distortion performance. Here we discuss some limitations of this work and point to possible solutions for future works.

Although our method has certain capability of scalability, it only supports a 2-stage scalable coding and rendering. It may be desirable to achieve a more fine-grained scalability between level 9 and 10 in an actual streaming application with adequate bandwidth. This can be potentially achieved by a region-adaptive coding scheme, which allocates more bits and produces more Gaussians in areas where more points are present. This is also promising for reducing the decoding / rendering latency towards a real-time system.

On the other hand, we observe that the existing 3D Gaussian rasterizer tends to lower the texture contrast (compared to the ground truth) due to the alpha blending mechanism. An earlier work [35] shows that this can be resolved by carefully handling the intersection region of two Gaussians. By improving the differential renderer, we may also be able to boost the R-D performance and visual quality.

6 Conclusion

To address the critical roadblock in using point cloud for real-time volumetric video streaming, we propose a novel point cloud compression scheme, Bits-to-

Photon (B2P), which jointly designs a scalable color compression scheme and a decoder to directly generate 3D Gaussian parameters for rendering. Leveraging a differentiable Gaussian splatting renderer, we perform end-to-end optimization considering both compression ratio and rendering quality. We show that B2P achieves better bit-rate vs. rendering-quality performance than the state-of-the-art methods, while substantially reducing decoding and rendering latency. We believe that B2P opens an avenue of point cloud compression optimized for rendering, and is a promising step towards developing real-time 6-DoF volumetric streaming systems.

References

1. Mpeg g-pcc tmc13 (2023), <https://github.com/MPEGGroup/mpeg-pcc-tmc13>, accessed on Jan 24, 2024.
2. Aliev, K.A., Sevastopolsky, A., Kolos, M., Ulyanov, D., Lempitsky, V.: Neural point-based graphics. In: ECCV. pp. 696–712. Springer (2020)
3. Ballé, J., Minnen, D., Singh, S., Hwang, S.J., Johnston, N.: Variational image compression with a scale hyperprior. arXiv preprint arXiv:1802.01436 (2018)
4. Chang, J.H.R., Chen, W.Y., Ranjan, A., Yi, K.M., Tuzel, O.: Pointersect: Neural rendering with cloud-ray intersection. In: Proceedings of the IEEE/CVF Conference on Computer Vision and Pattern Recognition. pp. 8359–8369 (2023)
5. Chen, A., Mao, S., Li, Z., Xu, M., Zhang, H., Niyato, D., Han, Z.: An introduction to point cloud compression standards. *GetMobile: Mobile Computing and Communications* **27**(1), 11–17 (2023)
6. Choy, C., Gwak, J., Savarese, S.: 4d spatio-temporal convnets: Minkowski convolutional neural networks. In: CVPR. pp. 3075–3084 (2019)
7. Cui, M., Long, J., Feng, M., Li, B., Kai, H.: Octformer: Efficient octree-based transformer for point cloud compression with local enhancement. In: Proceedings of the AAAI Conference on Artificial Intelligence. vol. 37, pp. 470–478 (2023)
8. d’Eon, E., Bob, H., Myers, T., Chou, P.A.: 8i voxelized full bodies - a voxelized point cloud dataset. In: ISO/IEC JTC1/SC29 Joint WG11/WG1 (MPEG/JPEG) input document WG11M40059/WG1M74006 (2017)
9. Fang, G., Hu, Q., Wang, H., Xu, Y., Guo, Y.: 3dac: Learning attribute compression for point clouds. In: CVPR (2022)
10. Fu, C., Li, G., Song, R., Gao, W., Liu, S.: Octattention: Octree-based large-scale contexts model for point cloud compression. In: Proceedings of the AAAI Conference on Artificial Intelligence. vol. 36, pp. 625–633 (2022)
11. Graziosi, D., Nakagami, O., Kuma, S., Zaghetto, A., Suzuki, T., Tabatabai, A.: An overview of ongoing point cloud compression standardization activities: Video-based (v-pcc) and geometry-based (g-pcc). *APSIPA Transactions on Signal and Information Processing* **9**, e13 (2020)
12. Han, B., Liu, Y., Qian, F.: Vivo: Visibility-aware mobile volumetric video streaming. In: Proceedings of the 26th annual international conference on mobile computing and networking. pp. 1–13 (2020)
13. He, K., Zhang, X., Ren, S., Sun, J.: Deep residual learning for image recognition. In: Proceedings of the IEEE conference on computer vision and pattern recognition. pp. 770–778 (2016)
14. He, Y., Ren, X., Tang, D., Zhang, Y., Xue, X., Fu, Y.: Density-preserving deep point cloud compression. In: CVPR (2022)

15. Huang, L., Wang, S., Wong, K., Liu, J., Urtasun, R.: Octsqueeze: Octree-structured entropy model for lidar compression. In: CVPR. pp. 1313–1323 (2020)
16. Huang, Y., Peng, J., Kuo, C.C.J., Gopi, M.: Octree-based progressive geometry coding of point clouds. In: PBG@ SIGGRAPH. pp. 103–110 (2006)
17. Kazhdan, M., Hoppe, H.: Screened poisson surface reconstruction. TOG **32**(3), 1–13 (2013)
18. Kerbl, B., Kopanas, G., Leimkühler, T., Drettakis, G.: 3d gaussian splatting for real-time radiance field rendering. ACM Transactions on Graphics **42**(4) (2023)
19. Lee, K., Yi, J., Lee, Y., Choi, S., Kim, Y.M.: Groot: a real-time streaming system of high-fidelity volumetric videos. In: Proceedings of the 26th Annual International Conference on Mobile Computing and Networking. pp. 1–14 (2020)
20. Mao, Y., Hu, Y., Wang, Y.: Learning to predict on octree for scalable point cloud geometry coding. In: 2022 IEEE 5th International Conference on Multimedia Information Processing and Retrieval (MIPR). pp. 96–102. IEEE (2022)
21. Nakagami, O., Lasserre, S., Toshiyasu, S., Preda, M.: White paper on g-pcc. In: ISO/IEC JTC 1/SC 29/AG 03 N0111 (2023), https://www.mpeg.org/wp-content/uploads/mpeg_meetings/142_Antalya/w22804.zip
22. Que, Z., Lu, G., Xu, D.: Voxelcontext-net: An octree based framework for point cloud compression. In: CVPR. pp. 6042–6051 (2021)
23. Sheng, X., Li, L., Liu, D., Xiong, Z., Li, Z., Wu, F.: Deep-pcac: An end-to-end deep lossy compression framework for point cloud attributes. IEEE Transactions on Multimedia **24**, 2617–2632 (2021)
24. Thomas, H., Qi, C.R., Deschaud, J.E., Marcotegui, B., Goulette, F., Guibas, L.J.: Kpconv: Flexible and deformable convolution for point clouds. In: ICCV. pp. 6411–6420 (2019)
25. Wang, J., Ding, D., Li, Z., Feng, X., Cao, C., Ma, Z.: Sparse tensor-based multi-scale representation for point cloud geometry compression. IEEE Transactions on Pattern Analysis and Machine Intelligence (2022)
26. Wang, J., Ma, Z.: Sparse tensor-based point cloud attribute compression. In: 2022 IEEE 5th International Conference on Multimedia Information Processing and Retrieval (MIPR). pp. 59–64. IEEE (2022)
27. Wang, J., Zhu, H., Liu, H., Ma, Z.: Lossy point cloud geometry compression via end-to-end learning. IEEE Transactions on Circuits and Systems for Video Technology **31**(12), 4909–4923 (2021)
28. Wang, Y., Sun, Y., Liu, Z., Sarma, S.E., Bronstein, M.M., Solomon, J.M.: Dynamic graph cnn for learning on point clouds. TOG **38**(5), 1–12 (2019)
29. Yifan, W., Serena, F., Wu, S., Öztireli, C., Sorkine-Hornung, O.: Differentiable surface splatting for point-based geometry processing. TOG **38**(6), 1–14 (2019)
30. Yu, T., Zheng, Z., Guo, K., Liu, P., Dai, Q., Liu, Y.: Function4d: Real-time human volumetric capture from very sparse consumer rgb-d sensors. In: CVPR (2021)
31. Zhang, J., Chen, T., Ding, D., Ma, Z.: Yoga: Yet another geometry-based point cloud compressor. In: Proceedings of the 31st ACM International Conference on Multimedia (2023)
32. Zhang, R., Isola, P., Efros, A.A., Shechtman, E., Wang, O.: The unreasonable effectiveness of deep features as a perceptual metric. In: CVPR. pp. 586–595 (2018)
33. Zhou, Q.Y., Park, J., Koltun, V.: Open3d: A modern library for 3d data processing. arXiv preprint arXiv:1801.09847 (2018)
34. Zwicker, M., Pfister, H., Van Baar, J., Gross, M.: Surface splatting. In: Proceedings of the 28th annual conference on Computer graphics and interactive techniques. pp. 371–378 (2001)

35. Zwicker, M., Rasanen, J., Botsch, M., Dachsbacher, C., Pauly, M.: Perspective accurate splatting. In: Proceedings-Graphics Interface. pp. 247–254. No. CONF (2004)

Appendix

A Network Architecture

We provide details on the sparse 3D convolution-based network architecture used in our method. This includes the *Feature Convert* module, the *Feature Squeeze* module, the *Predictive Entropy Model*, the *Feature Reconstruct* module, and the *3D Gaussian Generation* module. Please refer to Fig. 2 (*Feature Convert, Feature Squeeze and Predictive Entropy Model*) and Fig. 3 (*3D Gaussian Generation*) in the main paper for how these modules are incorporated in the proposed compression scheme.

A.1 Building Blocks

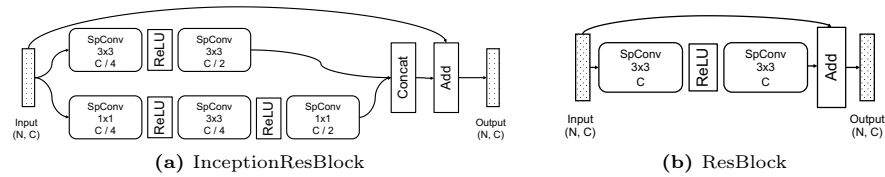


Fig. 7: The layer-wise details of the InceptionResBlock and ResBlock. *SpConv* is the abbreviation for 3D sparse convolution (Minkowski Convolution [6]). C is the number of input channels and N is the number of points in the input. The batch dimension is omitted for simplicity.

The proposed architecture includes two kinds of building blocks, *i.e.* InceptionResBlock and ResBlock. We adopt the InceptionResBlock architecture from the work [27]. For completeness, we also provide the detail in this section. The ResBlock is a 3D sparse version of the original residual block [13]. The layer-wise details of these two blocks are shown in Fig. 7.

A.2 Feature Convert Module

Table 3: The architecture of the *Feature Convert* module.

Layer	Layer Type	Input Channel	Output Channel	Kernel Size	Activation
1	Geom-Invariant 3D Conv.	C_{in}	64	3×3	None
2	InceptionResBlock	64	64	-	ReLU
3	InceptionResBlock	64	64	-	ReLU
4	Geom-Invariant 3D Conv.	64	64	3×3	None

The *Feature Convert* module architecture shown in Table 3 is used for both extracting feature from the input point cloud (RGB colors as features) or converting a down-sampled point cloud with features from a denser level to features for this level. The output will 1) go to the *Feature Squeeze* module for further processing, and 2) be down-sampled to the next level for further processing by another *Feature Squeeze* module.

A.3 Feature Squeeze Module

Table 4: The architecture of the *Feature Squeeze* module.

Layer	Layer Type	Input Channel	Output Channel	Kernel Size	Activation
1	Per-point Linear Layer	64 + 64	64	1 × 1	ReLU
2	Per-point Linear Layer	64	8	1 × 1	None

The *Feature Squeeze* module architecture shown in Table 4 is used for reducing the dimensionality of the features at this level. Since we want to remove the predictable information to save bit-rates, we design the process to be conditioned on the up-sampled feature from a coarser level. Hence, the input layer in Table 4 has 64 + 64 input channels, corresponding to the features at this layer and the context from a coarser layer, respectively. The output will be quantized and entropy coded, with a *Predictive Entropy Model*.

A.4 Predictive Entropy Model

Table 5: The architecture of the *Predictive Entropy Model* module.

Layer	Prev.	Layer Type	Input Channel	Output Channel	Kernel Size	Activation
1	-	Geom-Invariant 3D Conv.	64	64	3 × 3	ReLU
2	1	Geom-Invariant InceptionResBlock	64	64	-	ReLU
3	2	Geom-Invariant InceptionResBlock	64	64	-	ReLU
4	3	Per-point Linear Layer	64	8	1 × 1	None
5	3	Per-point Linear Layer	64	8	1 × 1	Exp

The *Predictive Entropy Model* architecture shown in Table 5 is used for modeling the conditional entropy of the quantized features. We assume the squeezed features follow a conditional Gaussian distribution. The *Feature Squeeze* module thus takes the upsampled feature from a coarser level as input, and generates the mean and scale of the Gaussian distribution for each point, which is used to form the cumulative distribution function (CDF) for entropy coding. In Table 5,

Layer 4 generates the mean μ while Layer 5 generates the scale σ . The output will be used for entropy coding the quantized features from the *Feature Squeeze* module.

A.5 Feature Reconstruct Module

Table 6: The architecture of the *Feature Reconstruct* module.

Layer	Layer Type	Input Channel	Output Channel	Kernel Size	Activation
1	Per-point Linear Layer	8 + 64	64	1×1	ReLU
2	InceptionResBlock	64	64	-	ReLU
3	InceptionResBlock	64	64	-	ReLU
4	Per-point Linear Layer	64	64	1×1	None

The *Feature Reconstruct* module architecture shown in Table 6 is for reconstructing the higher dimensional feature from the squeezed and quantized features given by the *Feature Squeeze* module. Since the squeezing removes the predictable information, in the reconstruction the module should take the up-sampled feature from a coarser level as a conditioning input to reconstruct the features. The output will be used 1) as a conditioning input for coding a denser level, and 2) by the *3D Gaussian Generation* module to generate the renderable 3D Gaussians.

A.6 3D Gaussian Generation

Table 7: The architecture of the *3D Gaussian Generation* module.

Layer	Layer Type	Input Channel	Output Channel	Kernel Size	Activation
1	Geom-Invariant Conv.	64	64	3×3	ReLU
2	ResBlock	64	64	-	ReLU
3	ResBlock	64	64	-	ReLU
4	Geom-Invariant Conv. or 3D Transposed Conv.	64	64	2×2	None
5	ResBlock	64	64	-	ReLU
6	ResBlock	64	64	-	ReLU
7	Geom-Invariant Conv.	64	14	3×3	None

The *3D Gaussian Generation* module architecture shown in Table 7 is for generating the renderable 3D Gaussians from the reconstructed features. If this module is used at a coarse level (level 8 in our experiments), the 4th layer in Table 7 will be a 3D transposed convolution, which generates 8 times more points than the input for finer details. If this module is used at a denser level (level 9 in our experiments), the 4th layer in Table 7 is configured as a Geometry-Invariant 3D convolution, which generates the same number of points as the

input. The output includes 14 channels for the 3D Gaussian parameters, *i.e.* $\mu_x, \mu_y, \mu_z, \sigma_x, \sigma_y, \sigma_z, q_w, q_x, q_y, q_z, o, c$.

B Discussion on Point Cloud Video Compression and Rendering

In this section, we discuss a promising extension of our method to point cloud video compression and rendering. We conduct this experiment with the SiVFB dataset [8]. We compare our method to the standard scheme, which employs G-PCC for point cloud compression and OpenGL for rendering. Please kindly refer to the supplementary video for a demonstration of results.

As shown, our method is able to achieve a better quality at a lower bit-rate compared to the standard scheme. More importantly, when we look closer to the 3D surface, the holes / gaps between points will be visible in the standard scheme, which degrade the visual quality. In contrast, our method produces 3D Gaussians that approximate the smooth surface. Therefore, it does not suffer from the same issue and shows less visual artifacts.

Nevertheless, since the main focus of this paper is on joint point cloud compression and rendering for one frame, our method does have limitations in point cloud video compression and rendering. For example, we didn't consider the temporal coherence between frames, which is important for both compression and reconstruction. We notice some flickering effects in the rendered video, which is caused by the lack of temporal coherence. We believe that our method can be extended to point cloud video compression and rendering by incorporating temporal consistency loss and temporal modeling designs. For example, we can use warped previous frames as a conditioning input for the *Feature Squeeze* and *Feature Reconstruct* modules to reduce the bit-rates. We can also use this information to improve the temporal coherence in the rendering process, forming spatio-temporal 4D Gaussians. We leave these extensions as a promising future work.